Supporting Information

Falace et al. 10.1073/pnas.1316294111

SI Materials and Methods

RNA Interference Constructs. RNAi experiments were conducted with two shRNAs targeting the coding sequence (CDShp; nucleotides 407–427) or the 3′UTR (3′UTRhp; nucleotides 2259–2279) of *Rattus norvegicus* Tbc1 domain family member 24 (*Tbc1d24*) mRNA (GenBank accession no. NM_001105769.1). These constructs were designed using the siRNA Target Designer software (Promega Corporation, Madison, WI). BLAST searches against rat databases confirmed the specificity of each target. As negative controls, we used two corresponding nontargeting shRNAs (CDSm4hp and 3′UTRm4hp) with the same nucleotide sequence except in four positions. These shRNAs were subcloned into a mU6pro vector (gift from J. LoTurco, University of Connecticut, Storrs, CT) and then transfected into primary cortical neurons by Nucleofection (Amaxa) to text their knockdown efficiency.

Expression Constructs. For rescue experiments, we subcloned the coding sequence of human TBC1D24 (hTBC1D24) cDNA without the UTRs into the pCAGIG-IRES-enhanced green fluorescent protein (EGFP) vector (Addgene). Point mutations were introduced in hTBC1D24 by using the QuikChange site-directed mutagenesis kit (Stratagene) on the parent pCAGIG-hTBC1D24-EGFP vectors and confirmed by Sanger sequencing. Human ADP ribosylation factor (ARF)6^{T27N} and $ARF6^{Q67L}$ cDNAs were excised from pBME-$ARF6^{T27N}$ or pBME-$ARF6^{Q67L}$ vector (Biomatik), respectively, and subcloned into pCAGIG-IRES-EGFP. All constructs were verified by sequencing. Site-directed mutagenesis of *TBC1D24* were carried out using the following primers: D147H, 5′-CTGCACTACAGCATCCACGAGGCCGAGTGC-3′; F251L, 5′-TGGCCATCCTCAAGTCCTTCCACAAGGTGA-3′. Plasmid solutions were prepared using the EndoFree plasmid purification kit (Qiagen).

Western Blotting. Embryonic and postnatal brains were dissected and homogenized in lysis buffer [150 mM NaCl, 20 (mg/mL; 2%) SDS, 2 mM EDTA, Hepes 10 mM (pH 7.4), 0.2 mM phenylmethylsulfonyl fluoride, 2 μg/mL pepstatin, and 1 μg/mL leupeptin] using a tight-fitting Potter-Elvehjem homogenizer. Protein concentration was evaluated by bicinchoninic acid assay (Pierce). Twenty micrograms of protein extract were separated by SDS/PAGE, transferred to nitrocellulose, and immunoblotted with antibodies against TBC1D24 (1/1000; Aviva System Biology) and actin (1/5000; Sigma-Aldrich), followed by horseradish peroxidase-conjugated secondary antibodies (Bio-Rad). Signals were detected using the ECL chemiluminescence reaction (Pierce). Protein lysates from neuronal cultures and HeLa cells were extracted in lysis buffer [50 mM Tris (pH 7.5), 150 mM NaCl, 0.1% SDS, 1% Nonidet P-40, 0.2 mM phenylmethylsulfonyl fluoride, 2 μg/mL pepstatin, and 1 μg/mL leupeptin] and then separated by SDS/PAGE and assayed by immunoblotting with the following primary antibodies: anti-TBC1D24 (1/1000; Aviva System Biology), anti-ARF6 (1/1000; Sigma-Aldrich), and anti-actin (1/5000; Sigma-Aldrich).

In Utero Electroporation. Wistar rats (Janvier) were mated, cared for, and used in our animal facilities in agreement with the European Union and French legislations. Timed pregnant rats [embryonic day (E) 15; E0 was defined as the day of confirmation of sperm-positive vaginal plug] were anesthetized with a mixture of ketamine (10 mg/kg)/xylazine (100 mg/kg). The uterine horns were exposed, and a lateral ventricle of each embryo was injected using pulled glass capillaries and a microinjector (Picospritzer II; General Valve) with Fast Green (2 mg/mL; Sigma) combined with the following DNA constructs: 0.5 mg/mL pCAGGS-EGFP either alone or with 1.5 mg/mL shRNA construct targeting the TBC1D24 mRNA. Plasmids were further electroporated by discharging a 4,000 mF capacitor charged to 50 V with a BTX ECM 830 electroporator (BTX Harvard Apparatus). The voltage was discharged in five electrical pulses at 950-ms intervals via 5-mm electrodes placed on the head of the embryo across the uterine wall. Control and experimental embryos were obtained from the same litter, and the injections were made on the left and right ventricles, respectively, for later identification. We performed in utero electroporation (IUE) in embryonic rats at E15, corresponding to an active period of both radial and tangential migration of newborn neurons in the cortex.

Immunostaining Procedures. For immunostaining, rat brains were fixed (E17 or E20) or perfused [postnatal day (P) 7] with Antigenfix solution and sliced at 100 μm on a vibratome (Microm). Slices were blocked at room temperature (RT) for 1 h with 5% normal goat serum and 0.3% Triton X-100 in Phosphate buffered saline (PBS) and incubated overnight at 37 °C with the appropriate antibody for cell proliferation [Ki67 (Chemicon, 1/300) and phospho-histone H3 (PH3) (Millipore, 1/500)], for neuronal differentiation [TuJ1 (β-III tubulin; Promega; 1/6,000), FOXP2 (Abcam; 1/4,000), CDP (M-222 Santa Cruz Biotechnology; 1/200), Neu-N (Millipore; 1/300), and Vimentin (Millipore; 1/300)], and for cell death [Caspase3-Asp175 (Cell Signaling; 1/200)]. Sections were imaged on a laser-scanning confocal microscope (FluoView 300; Olympus). For immunocytochemistry, cells were grown on glass coverslips coated with poly-L-lysine (0.1 mg/mL; Sigma). Cells were fixed in 4% paraformaldehyde for 20 min at 37 °C and rinsed three times in PBS. Cells were subsequently incubated in blocking solution (0.1% Triton X-100, 1.5% nonfat dried milk in PBS) for 1 h at 37 °C and then incubated for 3 h at RT with polyclonal anti-vesicular glutamate transporter 1 (VGLUT1) antibody (1/1,000; Synaptic System) diluted in blocking solution. Cells were then washed three times with PBS before incubation with an AlexaFluor 594-conjugated anti-rabbit secondary antibody for 1 h at RT. After three washes in PBS, coverslips were mounted in Vectashield Hard Set Mounting Medium with 4′,6′-diamidino-2-phenylindole (Vector Laboratories). Sections were imaged on a laser-scanning confocal microscope (FluoView 300; Olympus). Images were processed using Photoshop software (Adobe Systems).

Quantitative Analysis. ***Neuronal migration.*** Quantification of neuronal migration was performed with the eCELLence software (www.gvt.it/ecellence) on E17, E20, and P7 coronal sections (100 μm) located in the dorsolateral neocortex as previously described (1). Confocal images of 50-μm-thick z-stacks were acquired and the Z-series of images were projected onto 2D representations, and three sections per mouse were analyzed. Relative positions of transfected cells were estimated by counting EGFP-positive cells in eight areas of interest normalized in individual sections to fit within the whole thickness of the cortex. For neuronal migration analysis at E17 and E20, the cortex was divided in three main regions corresponding to the ventricular zone (VZ) (strata 1 and 2), the intermediate zone (IZ) (strata 3–5), and the cortical plate (CP) (strata 6–8). At postnatal stages, layers II/IV and V/VI were visualized by labeling cortices with

CDP and FoxP2 antibody, respectively, and the relative positions of transfected GFP^+ cells in the cortical wall were quantified.

Cell cycle progression. We counted the number of EGFP-positive and $EGFP^+/Ki67^+$ cells or EGFP-positive and $EGFP^+/PH3$ cells in a defined area of 0.21 mm^2 (Adobe Photoshop-CS4) within the VZ of three confocal optical sections per embryo.

Morphological analysis. Images of EGFP fluorescence were acquired on a confocal laser-scanning microscope equipped with a 60× oil-immersion objective, and Z-series (15-μm-thick z-stacks) were projected to 2D representations. For analysis of neuronal polarization, sections were analyzed at E20, 5 d after electroporation. Cells were visualized by coexpressing EGFP, and the number of cells with multipolar, round, or normal bipolar morphology was counted in the upper part of the IZ (uIZ) (Adobe Photoshop-CS4/Image Pro Plus). Multipolar cells were defined as cells with more than three processes or polygonal morphology. Bipolar cells were considered as normal-locomoting neurons. All parameters for image acquisition were kept constant, with emission levels below saturation. For morphometric analysis, confocal images (50- to 70-μm-thick z-stacks) of isolated layer II/III pyramidal neurons and primary cortical neurons were acquired with a 40× oil-immersion objective, and Z-series were projected to 2D representations and used to sketch the neurite arbor. Quantification of dendritic length was performed after neuronal reconstructions with the ImageJ plug-in NeuronJ 1.2 software (2). A minimum of 80 neurons from four rats per condition were analyzed and various parameters were evaluated and compared (total dendrite length, apical and basal dendrite length).

Synapse quantification. To measure excitatory synapses primary neurons transfected at 13 d in vitro (DIV) and fixed 48–72 h posttransfection were labeled with the anti-VGLUT1 antibody. Images were acquired with Olympus 1 × 81 epifluorescence microscope equipped with a 100× oil objective using a constant exposure. Identical threshold were applied and an automatic count was performed with Image Pro Plus; 30–50 cells for each condition were analyzed from at least three independent preparations. For the analysis of axodendritic synapses, one or two of the thickest dendrites in each neuron were chosen, and VGLUT1-positive puncta 100 μm distal from the soma were selected. For somatic VGLUT1 cluster detection, images were manually thresholded, and analysis was conducted in the somatic region using Adobe Photoshop-CS4.

Cell Culture and Transfection. HeLa cells were maintained at 37 °C in a humidified 5% (vol/vol) CO_2 incubator in DMEM (Invitrogen) supplemented with 10% (wt/vol) FBS, 1 mM L-glutamine, and 4500 mg/L D-glucose. Cells were transfected with Lipofectamine 2000 (Life Technologies) according to the manufacturer's instructions. Primary cortical neurons were prepared from brains E18 brains of Sprague–Dawley rats as described (3); 3′UTRm4hp or 3′UTRhp combined with the pCAGGS-EGFP or pCAGIG-hTBC124-EGFP constructs were used for transfection. Neurons were transfected at time of plating by Nucleofection (Amaxa) and for later transfection (13–14 DIV) neurons using Lipofectamine 2000 (Life Technologies).

Electrophysiological Recordings. Patch electrodes, fabricated from thick borosilicate glasses (Hilgenberg), were pulled and fire-polished to a final resistance of 3–5 MΩ. Patch-clamp recordings were performed in whole-cell configuration using an Axon Multiclamp 700B/Digidata1440A system and pClamp 9.2 software (Molecular Devices). Miniature excitatory postsynaptic currents (mEPSCs) were acquired at 10-kHz sample frequency and filtered at 2 kHz with an eight-pole low-pass Bessel filter. Recordings with either leak currents >100 pA or a series resistance >15 MΩ were discarded. Series resistance was monitored throughout the experiment, and whenever it changed more than 15%, the recording was not included in the analysis. mEPSC recordings were performed on 17–18 DIV neurons at a holding potential of −70 mV in the presence of 50 μM D-2-amino-5-phosphonovaleric acid and 0.5 μM TTX (all from Tocris Bioscience) using an extracellular solution containing the following (in mM): 2 CaCl2, 140 NaCl, 1 MgCl2, 10 Hepes, 4 KCl, and 10 glucose (pH 7.3). The internal solution contained the following (in mM): 126 K gluconate, 4 NaCl, 1 $MgSO_4$, 0.02 CaCl2, 0.1 bis(2-aminophenoxy)ethane-N,N,N′,N′-tetraacetic acid, 15 glucose, 5 Hepes, 3 ATP, and 0.1 GTP (pH 7.3). Data analysis was performed by using the Minianalysis program (Synaptosoft). The amplitude and frequency of mEPSCs were calculated using a peak detector function with a threshold amplitude and a threshold area at 5 pA and 10 ms·pA, respectively. All experiments were performed at RT.

Cellular ARF6-Activation Assay. ARF6 activation in HeLa cells was determined using an ARF6-GTP–specific pull-down assay (4). HeLa cells were cotransfected with ARF6-HA and the indicated plasmid with Lipofectamine 2000 (Life Technologies); 24–30 h posttransfection, cells were lysed in ARF6 lysis buffer [50 mM Tris (pH 7.4), 100 mM NaCl, 2 mM MgCl2, 1% Nonidet P-40, 10% (vol/vol) glycerol, and 1 mM DTT plus protease inhibitors] and pelleted at 16,000 × *g* for 5 min at 4 °C. An aliquot of the clarified supernatant was taken directly for immunoblotting. The remainder was incubated with GST-Golgi-localized, gamma ear-containing, ARF-binding protein 3 (GGA3) (20–25 μg) conjugated to glutathione–Sepharose for 30 min at 4 °C. Beads were washed three times in ARF6 lysis buffer. Samples were fractionated by SDS/12% PAGE, and ARF6-GTP levels were evaluated by Western blotting using an anti-ARF6 antibody (Sigma-Aldrich).

1. Carabalona A, et al. (2012) A glial origin for periventricular nodular heterotopia caused by impaired expression of Filamin-A. *Hum Mol Genet* 21(5):1004–1017.
2. Meijering E, et al. (2004) Design and validation of a tool for neurite tracing and analysis in fluorescence microscopy images. *Cytometry A* 58(2):167–176.
3. Banker G, Goslin K (1998) *Culturing Nerve Cells* (MIT Press, Cambridge, MA).
4. Santy LC, Casanova JE (2001) Activation of ARF6 by ARNO stimulates epithelial cell migration through downstream activation of both Rac1 and phospholipase D. *J Cell Biol* 154(3):599–610.

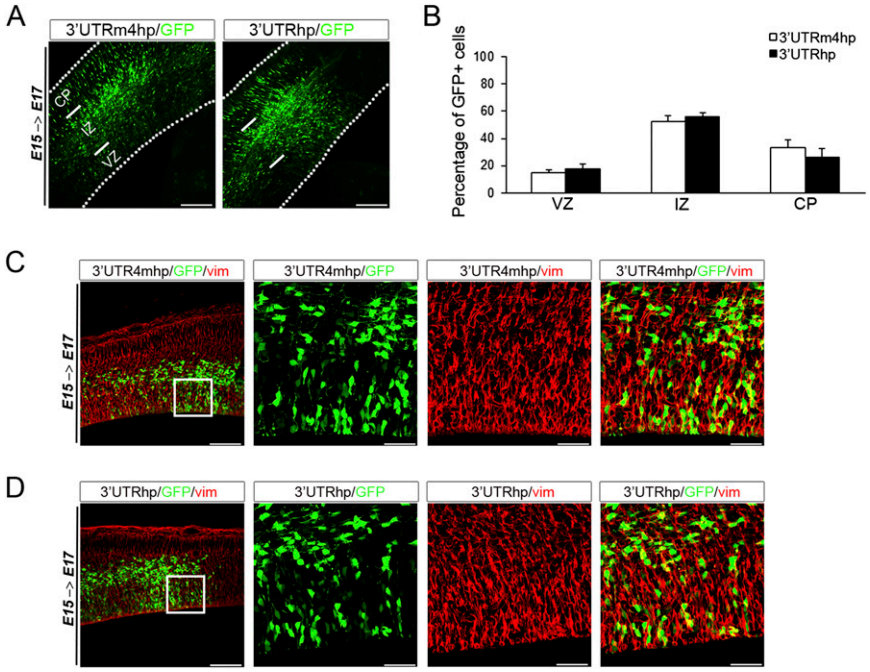

Fig. S1. TBC1D24 knockdown did not prevent radial migration out of the VZ/subventricular zone (SVZ). (*A*) Representative coronal sections of E17 rat brains 2 d after electroporation with indicated plasmids. (Scale bar: 200 μm.) (*B*) Quantification of GFP-positive cell distribution in the cortex expressed as a percentage of the total (3′UTRm4hp, $n = 6$; 3′UTRhp, $n = 5$). (*C* and *D*, *Left*) Representative coronal sections of E17 rat brains transfected at E15 with the indicated plasmids and immunostained for vimentin (vim). (Scale bar: 200 μm.) Boxed regions are shown on the right at high magnification. (Scale bar: 50 μm.)

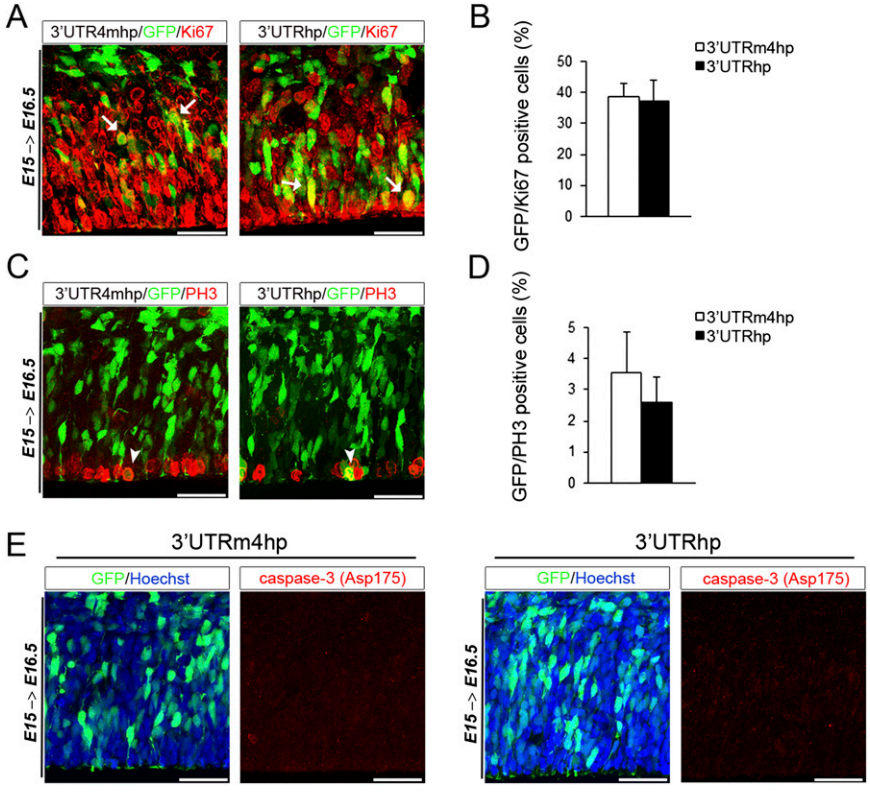

Fig. S2. TBC1D24 knockdown did not affect the cell cycle progression of neuronal progenitors or cell viability. (*A* and *C*) Representative confocal images of the VZ of rat cortices transfected at E15 with either the GFP vector combined with 3′UTRm3hp or with 3′UTRhp and immunostained 40–42 h later with the proliferation marker Ki67 or the mitotic nuclei marker PH3. Transfected cells positive for either marker appear in yellow (arrows in *A*; arrowhead in *C*). (Scale bar: 30 μm.) (*B* and *D*) Quantification (means ± SEM) of GFP and Ki67 (*B*) and GFP and PH3 (*D*) double-positive transfected cells in the VZ of independent brains (for Ki67, 3′UTRm4hp: $n = 12$; 3′UTRhp: $n = 11$; for PH3, 3′UTRm4hp: $n = 7$; 3′UTRhp: $n = 7$). (*E*) Immunostaining for cleaved activated caspase-3 (Asp175) shows no detectable elevation of apoptotic cell death in TBC1D24-knockdown brains 36 h after electroporation ($n = 4$ for each condition). (Scale bar: 30 μm.)

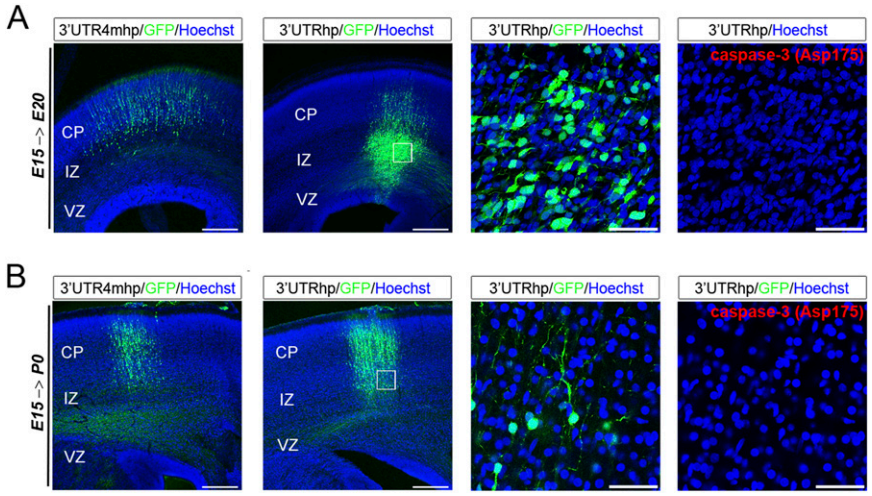

Fig. S3. Migration delay in the TBC1D24-knockdown brains does not induce apoptotic cell death. (*A* and *B*, *Left*) Representative coronal sections of E20 (*A*) and P0 (*B*) rat brains transfected at E15 with either 3′UTRm4hp or 3′UTRhp and counterstained with the chromosomal dye Hoechst to visualize cellular nuclei. (Scale bar: 200 μm.) Boxed regions are shown on the right at higher magnification. Immunostaining for cleaved activated caspase-3 (Asp175) shows no detectable apoptotic cell death in TBC1D24-knockdown neurons ($n = 3$ for each condition). (Scale bar: 30 μm.)

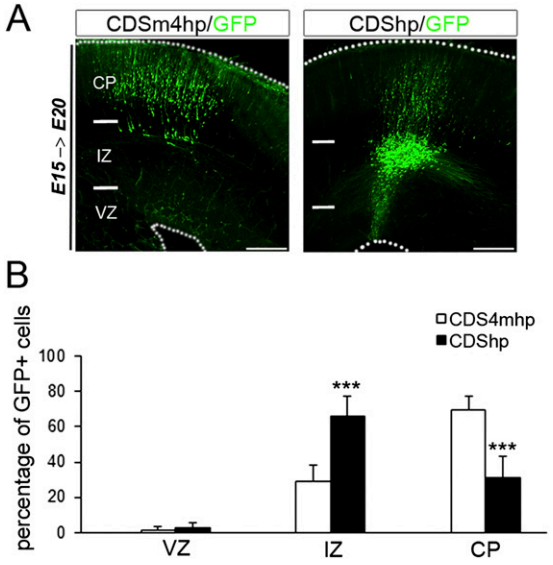

Fig. S4. In utero RNAi-mediated knockdown of TBC1D24 using CDShp alters radial migration. (*A*) Representative coronal sections of E20 rat brains 5 d after IUE at E15, showing the position of cells transfected with either the GFP construct combined with a shRNA construct targeting *TBC1D24* coding sequence (CDShp) or mutated shRNA (CDSm4hp). (Scale bar: 200 μm.) (*B*) Quantification of GFP-positive cell distribution in the cortex expressed as a percentage of the total. Data are expressed as means ± SEM and were compared via one-way analysis of variance (ANOVA) for repeated measure. ***$P < 0.001$ (CDShp $n = 8$; CDSm4hp $n = 8$).

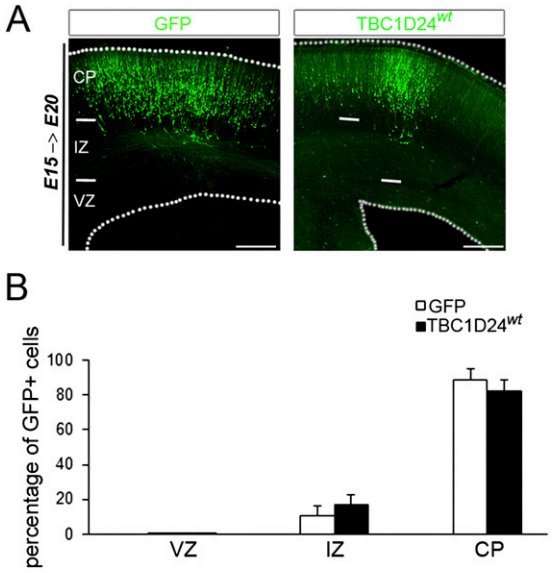

Fig. S5. Overexpression of TBC1D24 protein did not alter radial migration. (*A*) Representative coronal sections of E20 rat brains 5 d after electroporation at E15 with either GFP or TBC1D24^{wt} construct. (Scale bar: 200 μm.) (*B*) Quantification of GFP-positive cell distribution in the cortex expressed as a percentage of the total number of transfected cells (GFP, $n = 9$; TBC1D24^{wt}, $n = 6$).

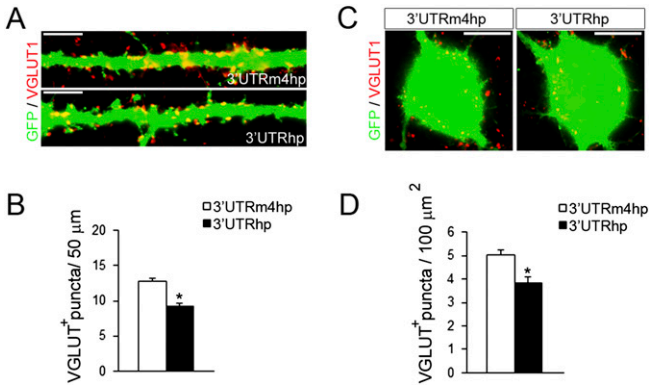

Fig. S6. Excitatory synapses formation is impaired in TBC1D24-knockdown neurons in vitro. (*A*) High-magnification images on dendritic tracts of 18 DIV cortical neurons transfected with GFP combined with either 3′UTRm4hp or 3′UTRhp and processed for VGLUT1 staining. (Scale bar: 10 μm.) (*B*) Quantitative analysis reveals a reduced number of axodendritic VGLUT1 puncta in the TBC1D24-knockdown neurons compared with control neurons. Data are expressed as means ± SEM from 65 to 72 neurons per each condition obtained from three independent preparations. (*C*) High-magnification images of somatic VGLUT1 staining in 18 DIV primary cortical neurons treated as in *A*. (Scale bar: 20 μm.) (*D*) Histogram showing the quantitative analysis of axosomatic synapses. Data are expressed as means ± SEM from three independent preparations (36–45 neurons per condition). Data were analyzed by paired two-tailed *t* test. $*P < 0.05$.

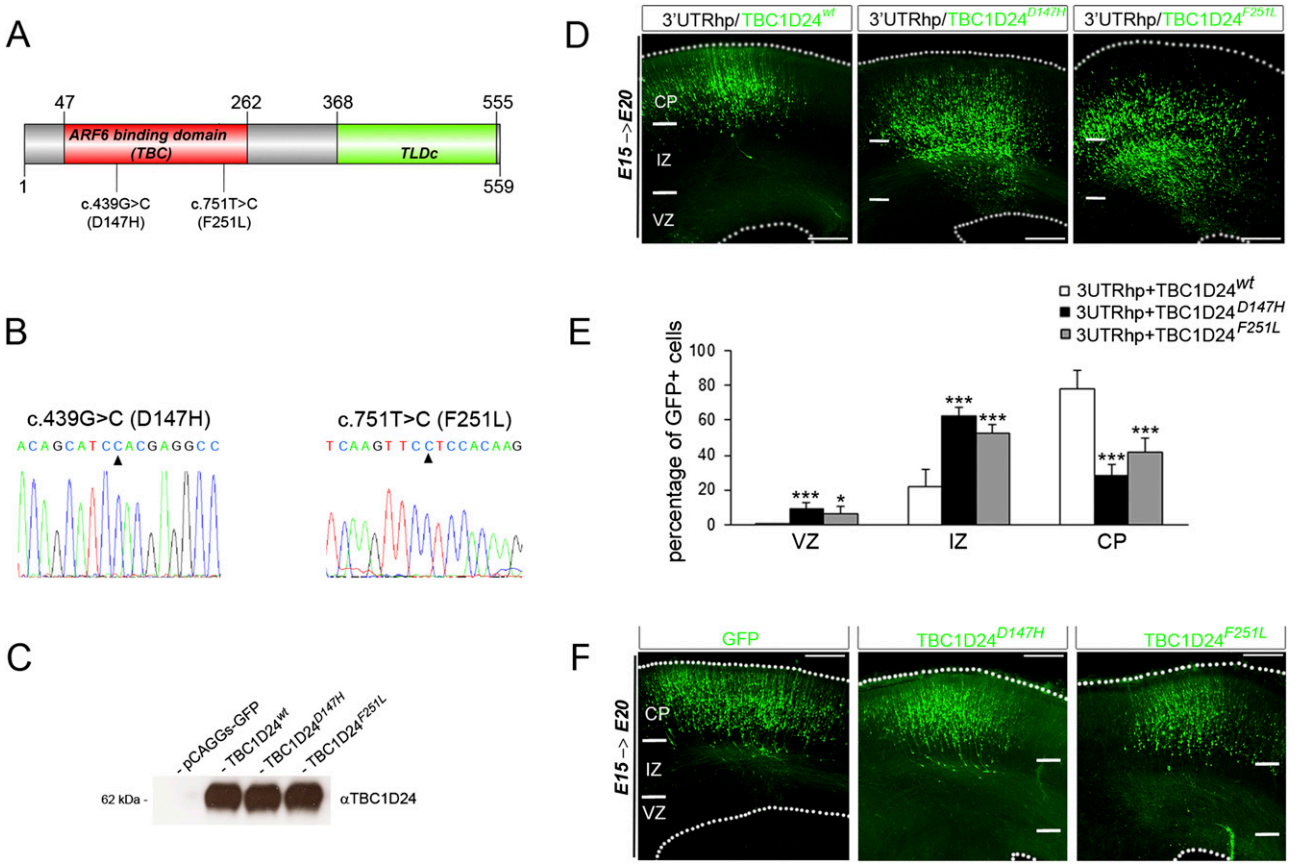

Fig. S7. TBC1D24 variants defective for ARF6 bindings fail to rescue the migration delay in the TBC1D24-knockdown model. (*A*) Graphic model of the conserved domains in the human TBC1D24 protein. TBC1D24 is characterized by a Tre2/Bub2/Cdc16 (TBC) domain enabling ARF6-binding and a TLDc domain with no reported function. Amino acid position for the D147H and F251L mutations are shown. (*B*) Electropherograms of c.439G > C (p.D147H) and c.751T > C (p.F251L) mutations introduced into the pCAGIG-hTBC1D24-EGFP construct. (*C*) Western blotting analysis of TBC1D24 constructs transfected in HeLa cells revealed with an anti-TBC1D24 antibody (α-TBC1D24) 36 h posttransfection. (*D*) Representative coronal sections of E20 rat brains 5 d after electroporation with 3′UTRhp and TBC1D24 constructs. (Scale bar: 200 μm.) (*E*) Quantification of GFP-positive cell distribution in the cortex expressed as a percentage of the total (3′UTRhp + TBC1D24^{wt}, $n = 9$; 3′UTRhp + TBC1D24^{D147H}, $n = 6$; 3′UTRhp + TBC1D24^{F251L}, $n = 6$). Data, expressed as means ± SEM, were compared using one-way ANOVA for repeated measures, followed by the Bonferroni's multiple comparison test. ***$P < 0.0001$ and *$P < 0.05$ vs. 3′UTRhp + TBC1D24^{wt}. (*F*) Representative coronal sections of E20 rat brains 5 d after electroporation at E15 with either GFP or TBC1D24 variants. (Scale bar: 200 μm.)

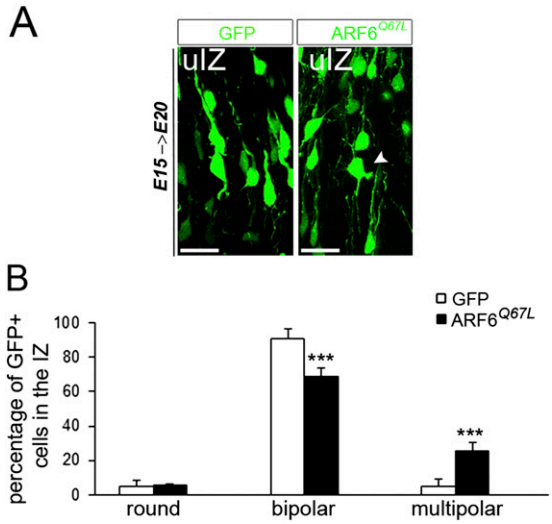

Fig. S8. Acquisition of bipolar morphology is impaired into ARF6^{Q67L}-overexpressing neurons. (*A*) High magnification (60×) of E20 rat cortices electroporated at E15 with control vector or ARF6^{Q67L} in the uIZ. (Scale bar: 20 μm.) Overexpression of ARF6^{Q67L} in migrating neurons impaired multipolar/bipolar transition (arrowhead). (*B*) Histogram showing average percentage of the polarity at level of the uIZ (control, $n = 7$; ARF6^{Q67L}, $n = 7$). Data, expressed as means ± SEM, were compared by one-way ANOVA for repeated measures. ***$P < 0.001$ vs. GFP.

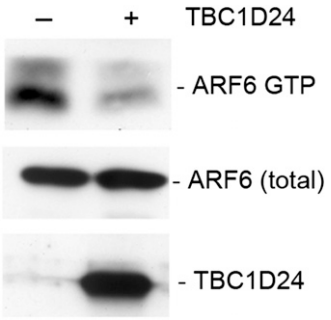

Fig. S9. Pull-down assay for ARF6 activity. Active GTP-bound ARF6 was precipitated with GST-GGA3 from lysates of HeLa cells coexpressing ARF6-HA and TBC1D24-IRES-GFP (+) or ARF6-HA alone (-) as control. ARF6-GTP is inhibited by TBC1D24 overexpression.

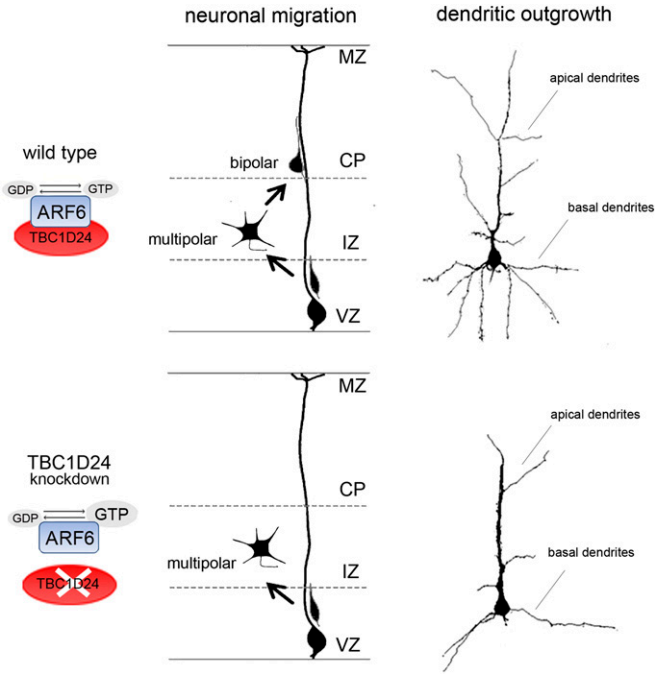

Fig. S10. Proposed model for the function of TBC1D24 in developing neurons. A tight TBC1D24-dependent control of ARF6 endocytic pathway is physiologically required during morphological changes underlying radial migration and functional maturation of cortical neurons. Loss of TBC1D24 would result in the dysregulation of ARF6 activity, which in turn impairs the multipolar-to-bipolar transition and the proper development of the dendritic tree.